periodica polytechnica

Mechanical Engineering
56/1 (2012) 43–47

web: http://www.pp.bme.hu/me

RESEARCH ARTICLE

Time-optimal computed-torque control in contact transitions

Bálint Magyar / *Gábor* Stépán

Received 2012-04-30

Abstract

The simple mechanical model of an approach-and-touch control procedure is discussed. The aim is to find an appropriate control strategy to approach the target surface, handle the contact transitions and apply the desired force on the contact surface. In the control loop, position and force feedback is present; the absolute position of the target surface is only available for the controller with limited accuracy.

Keywords

contact transition · piecewise-linear system · computed-torque · bang-bang

Bálint Magyar

Department of Applied Mechanics, BME, H-1111 Budapest, Műegyetem rkp. 5, Hungary

e-mail: magyar@mm.bme.hu

Gábor Stépán

Department of Applied Mechanics, BME, H-1111 Budapest, Műegyetem rkp. 5, Hungary

e-mail: stepan@mm.bme.hu

1 Introduction

It is a common task in robotics and computer-integrated manufacturing to approach and get in touch with an object, and then apply a desired contact force on the surface of the object. A typical problem is polishing, for example; there has been a considerable effort on developing advanced control strategies for this field of application (see e.g. [1], [2], [3], [4] and [5]). This procedure requires both position and force control, moreover, in most of the cases a compound of those, and besides the duality of control, mathematical description of approaching and touching an object results a piecewise discontinuous system (see e.g. [6] and [7]).

Sensory weighting of force and position feedback is an open problem in human motor control tasks as well. The coherence between sensory weighting and the stiffness of the object is investigated in [8]; the authors' assumption is that position feedback is weighted more in case of soft objects, while force feedback is weighted more in case of stiff objects. In [9], the authors attempt to find an optimal open-loop control strategy for transitioning from finger motion to static fingertip force production.

In this paper, three hypothetical phases of contact transitions are assumed. During the first phase of rough positioning, the manipulator is driven relatively close to the target surface. The corresponding distance between the manipulator and the object surface depends on a priori knowledge of the accuracy of the position detection, and it is chosen to satisfy the essential requirements of avoiding penetration or unwanted collision. Within this distance, the position feedback becomes unreliable and the control strategy has to be changed for the second phase of contact transition: the manipulator should approach the target surface with a reduced moderate velocity until contact is detected by the force sensor. In the third phase, the controller has to slow down the moving parts while tuning the applied contact force to the desired value at the end of the transition.

In the subsequent sections, we analyse phase two, approaching, and phase three, force control with the help of the corresponding mechanical models. The aim of the following investigation is to determine the maximum velocity that can be applied during the first phase of rough positioning with the assump-

tion of securing soft (inelastic-like) collision with the target and avoiding multiple contacts. In other words, an appropriate control strategy is developed for the approach-and-touch procedure that minimizes the time required for the approach of an object before it is touched.

2 Mechanical Model

The simplest non-trivial mechanical model is assumed that can be used to analyse the above described problem of approach-and-touch. This model consists of two rigid bodies connected by a linear spring and a linear viscous damper, as shown in Fig. 1. The mass m of the block represents the inertia of the manipulator system, the spring of stiffness k and the damper of damping coefficient c model the linear visco-elastic characteristics of the force sensory system. Dry friction is neglected everywhere, and the mass m_c of the bumper is assumed to be negligible, which means that its velocity becomes zero as it touches the wall. Still, this model can describe abrupt change of the contact force from zero as the bumper touches the wall, since the relative velocity between the two ends of the damper will become discontinuous, while the spring force will increase continuously from zero.

The state of the system is described by two coordinates, the absolute position of the block of mass m, and the position of the bumper relative to the block, which are x_1 and x_2, respectively. Since the absolute position of the target wall is only available with limited accuracy, the distance between the bumper and the wall at $x_1 = 0$ and $x_2 = 0$ appears as an offset $\delta \neq 0$. The block is driven by the control force Q. The instantaneous control force is computed by the controller based on computed torque control, on state feedback, or on the combination of the two. The aim of the procedure is to approach the target with the bumper, and to provide the desired constant force F_d in a fast and robust way without losing contact with the wall after it was touched once. Since the mass of the bumper is neglected, the Newtonian governing equations form a system of ordinary differential equations (ODEs), where the first is a second-order ODE for x_1 while the second is a first-order ODE for x_2 corresponding to a mechanical system of one and a half degrees of freedom (DoF).

The spring force kx_2 and the damping force $c\dot{x}_2$ depend on the relative position x_2 and relative velocity $\dot{x}_2$ of the bumper, respectively. If there is no contact between the bumper and the target, the following equations of motion are obtained:

$$m\ddot{x}_1 = kx_2 + c\dot{x}_2 + Q, \tag{1}$$

$$m_c(\ddot{x}_1 + \ddot{x}_2) = -kx_2 - c\dot{x}_2, \tag{2}$$

which become decoupled for $m_c = 0$), obviously, if the control force Q does not depend on the state variables x_2 and $\dot{x}_2$ of the force sensory system. These equations hold till the condition of getting in contact with the wall does not fulfil. The criterion of getting in contact with the wall is given with the help of the offset δ in the following form:

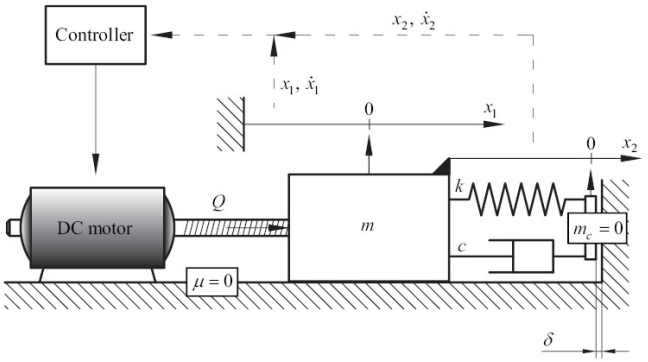

Fig. 1. Mechanical model of the approach-and-touch task.

$$x_1 + x_2 - \delta = 0. \tag{3}$$

During contact, the contact force $F_c > 0$ acting on the target is the resultant of the spring force and the damping force:

$$F_c = -kx_2 - c\dot{x}_2. \tag{4}$$

Consequently, the contact force will appear in the equation of motion of the block, but the actual mathematical form of the corresponding ODE remains the same as (1). In the meantime, the geometric constraint in (3) will be valid, which can also be reformulated as a kinematic constraint:

$$\dot{x}_2 = -\dot{x}_1, \tag{5}$$

and this remains true till the contact force is positive. After the introduction of the velocity of the block ($x_3 = \dot{x}_1$) with the standard Cauchy transformation, the corresponding discontinuous mathematical model is formed of two systems of three first-order ODEs:

$$\begin{pmatrix} \dot{x}_1 \\ \dot{x}_2 \\ \dot{x}_3 \end{pmatrix} = \begin{pmatrix} 0 & 0 & 1 \\ -k/c & 0 & 0 \\ 0 & 0 & 0 \end{pmatrix} \begin{pmatrix} x_1 \\ x_2 \\ x_3 \end{pmatrix} + \begin{pmatrix} 0 \\ 0 \\ Q/m \end{pmatrix}, \quad \text{if } x_2 + x_1 - \delta < 0 \tag{6}$$

for no contact, and:

$$\begin{pmatrix} \dot{x}_1 \\ \dot{x}_2 \\ \dot{x}_3 \end{pmatrix} = \begin{pmatrix} 0 & 0 & 1 \\ 0 & 0 & -1 \\ 0 & k/m & -c/m \end{pmatrix} \begin{pmatrix} x_1 \\ x_2 \\ x_3 \end{pmatrix} + \begin{pmatrix} 0 \\ 0 \\ Q/m \end{pmatrix}, \quad \text{if } kx_2 - cx_3 < 0 \tag{7}$$

for contact. In order to illustrate the behaviour of the uncontrolled system, simulations were carried out with constant driving force that equals to the desired contact force $Q(t) \equiv F_d$. Fig. 2 represents the results. It should be noted that even though the collision of the zero-mass bumper and the wall appears to be totally inelastic, multiple contacts (bouncing) can occur. In case of zero viscous damping coefficient $c = 0$, however, the collision of the rigid body system and the wall still looks perfectly elastic with periodic impacts of constant mechanical energy.

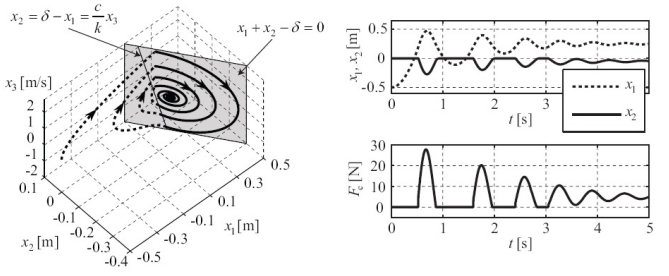

Fig. 2. Simulation results for constant driving force, parameters $m = 1$ kg, $k = 100$ N/m, $c = 2$ Ns/m, $Q(t) \equiv F_d = 5$ N, $\delta = 0.2$ m. Phase space (left), time history (right).

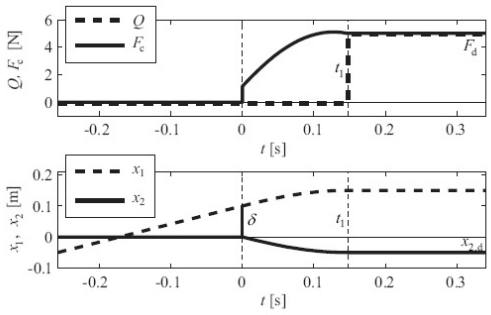

Fig. 3. Control strategy with one step, parameters $m = 1$ kg, $k = 100$ N/m, $c = 2$ Ns/m, $F_d = 5$ N, $x_{2,d} = -0.05$ m, $\delta = 0.1$ m, $t_1 = 0.148$ s, $v_a = 0.579$ m/s.

3 Optimization of the Computed Torque

As explained in the introduction, our goal is to maximize the velocity of approach applied during the rough positioning phase, while we are going to avoid multiple impacts to the target that serves as a constraint together with the saturation of the controller at control force magnitude Q_m. If we approach the target with maximum speed, the kinetic energy of the manipulator is maximized, too, and the maximum actuator force should be used (see [10]) to slow it down as fast as possible at the desired equilibrium state

$$x_1(t) \equiv \delta + F_d/k,\ x_2(t) \equiv x_{2,d} = -F_d/k. \tag{8}$$

This means that a kind of bang-bang computed-torque control will be applied with control force

$$Q(t) = -Q_m \operatorname{sgn}(\dot{x}_1). \tag{9}$$

Also, the maximum velocity of approach can be calculated offline from the condition that the system has to settle at the desired state (8) in a stable way.

In the following subsections different cases will be studied, depending on how many constant control force steps are implemented, starting with the simplest one-step scenario.

3.1 One-step Scenario

Consider the case, when the manipulator touches the target at the time instant $t_0 = 0$ but the controller is switched on only at an appropriate time instant t_1, that is, $Q(t) \equiv 0$ for $t < t_1$ and $Q(t) \equiv F_d$ for $t \in [t_1, \infty)$ leading to a standstill at the desired equilibrium. Fig. 3 represents this control scenario. Due to the zero-point offset, the contact occurs at $x_1(0) = \delta$. The corresponding velocity of approach v_a can be determined in the following way. The initial conditions are

$$x_2(0) = 0 \text{ and } \dot{x}_2(0) = -v_a, \tag{10}$$

consequently, the specific solution of (2) is

$$x_2(t) = -\frac{v_a}{\omega_d} e^{-\zeta\omega_n t} \sin(\omega_d t),\ t \in [t_0, t_1), \tag{11}$$

where the undamped natural angular frequency, the damped natural angular frequency and the damping ratio are:

$$\omega_n = \sqrt{\frac{k}{m}},\ \omega_d = \omega_n\sqrt{1-\zeta^2} \text{ and } \zeta = \frac{1}{2m\omega_n}, \tag{12}$$

respectively. The peak in (11) is at

$$t_1 = \frac{1}{\omega_d} \arctan\left(\frac{\sqrt{1-\zeta^2}}{\zeta}\right). \tag{13}$$

In order to bring the system to the desired equilibrium state, the peak value at t_1 has to be equal to the desired position $x_{2,d} = -F_d/k$. From (8), the velocity of approach can be expressed explicitly:

$$v_a = x_{2,d}\omega_n \exp\left(\frac{\zeta}{\sqrt{1-\zeta^2}} \arctan\left(\frac{\sqrt{1-\zeta^2}}{\zeta}\right)\right). \tag{14}$$

Its numerical value is $v_a = 0.579$ m/s for the data presented in Fig. 3. For $\zeta = 0$, the expression simplifies to

$$v_a = x_{2,d}\omega_n. \tag{15}$$

In the subsequent cases, more complicated scenarios will be considered where the velocity of approach is increased further, but the analytical calculations cannot be carried out explicitly in the same way as we did above for the one-step case.

3.2 Two-steps Scenario

In order to increase the velocity of approach, larger amount of kinetic energy is to be eliminated by the controller. Considering (9), the maximal braking force should be applied immediately after the contact is detected at $t_0 = 0$ until the time instant t_1 where the velocity $\dot{x}_2$ becomes zero:

$$Q(t) \equiv -Q_m,\ t \in [0, t_1),\ \dot{x}_2(t_1) = 0. \tag{16}$$

Then the same desired force $Q(t) \equiv F_d$ should be applied for $t \in [t_1, \infty)$, just as in the previous case. Fig. 4 illustrates this scenario.

Introduce the maximum static deformation of the spring by $f_0 = Q_m/k$. The initial conditions are the same as in (10) and the corresponding specific solution of (2) is

$$x_2(t) = f_0 - e^{-\zeta\omega_n t}\left(\frac{v_a + \zeta\omega_n f_0}{\omega_d} \sin(\omega_d t) + f_0 \cos(\omega_d t)\right), \tag{17}$$

The time instant t_1 can be calculated from the condition $\dot{x}_2(t_1) = 0$, where x_2 has a minimum:

$$t_1 = \frac{1}{\omega_d} \arctan\left(\frac{\omega_d v_a}{\omega_d^2 f_0 + \zeta\omega_n(\zeta\omega_n f_0 + v_a)}\right). \tag{18}$$

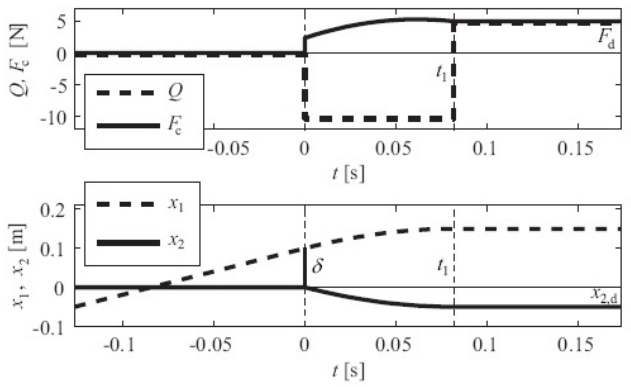

Fig. 4. Control strategy with two steps, parameters $m = 1$ kg, $k = 100$ N/m, $c = 2$ Ns/m, $F_d = 5$ N, $x_{2,d} = -0.05$ m, $\delta = 0.1$ m, $t_1 = 0.082$ s, $v_a = 1.188$ m/s.

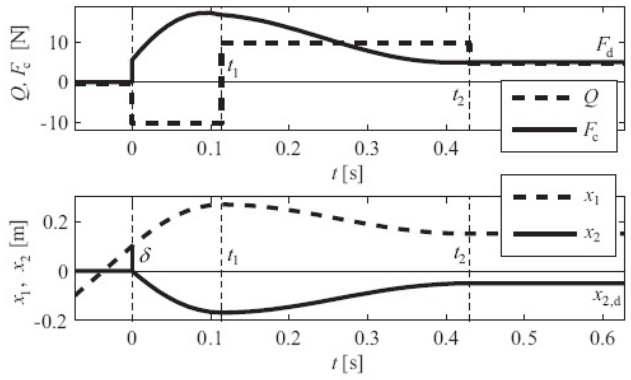

Fig. 5. Control strategy with three steps, parameters $m = 1$ kg, $k = 100$ N/m, $c = 2$ Ns/m, $F_d = 5$ N, $x_{2,d} = -0.05$ m, $\delta = 0.1$ m, $t_1 = 0.114$ s, $t_2 = 0.429$ s, $v_a = 2.741$ m/s.

This time, the velocity of approach v_a cannot be expressed in closed form from the condition $x_2(t_1) = x_{2,d}$, but any simple nonlinear solver can provide its numerical value. For the given parameters, the velocity of approach is increased from 0.579 m/s of the one-step-case to 1.188 m/s of the two-steps-case.

3.3 Three-step Scenario

If overshoot is permitted while the multiple impacts are still excluded, the control strategy can be extended with a third step (see Fig. 5), allowing a higher velocity of approach compared to the previous cases. The applied control force is $Q(t) \equiv -Q_m$ for $t \in [0, t_1)$ as in the previous case, but then $Q(t) \equiv Q_m$ for $t \in [t_1, t_2)$ and $Q(t) \equiv F_d$ for $t \geq t_2$ only, where t_1 and t_2 are the subsequent time instants when the velocity of the block is zero: $\dot{x}_2(t_1) = 0$ and $\dot{x}_2(t_2) = 0$.

Initial conditions for phase $t \in [t_0, t_1)$ are given in (10), and the specific solution for this interval is (17), as before. The condition $\dot{x}_2(t_1) = 0$ is valid for the three-steps scenario as well, and t_1 can be calculated according to (18).

In order to formulate the initial conditions for the phase $t \in [t_1, t_2)$, $x_2(t)_1$ can be calculated from (17) and (18), while $\dot{x}_2(t_1) = 0$ is prescribed. The specific solution for this interval is

$$x_2(t) = -f_0 + (x_2(t_1) + f_0)\, e^{-\zeta\omega_n(t-t_1)} \times \left(\frac{\zeta\omega_n}{\omega_d} \sin(\omega_d (t - t_1)) + \cos(\omega_d (t - t_1)) \right). \tag{19}$$

Since there is a half oscillation between t_1 and t_2, the time instant when the control force should be changed to F_d is at $t_2 = t_1 + \pi/\omega_d$ where t_1 comes from (18). Numerical solution of $x_2(t_2) = x_{2,d}$ can be carried out to determine v_a that ensures the arrival to the desired state of equilibrium (8). This value is increased further to 2.741 m/s.

3.4 Four-step Scenario

In order to determine the maximum allowed approaching velocity for which multiple impacts are avoided, an additional control step should be involved as illustrated in Fig. 6. The applied control force is $Q(t) \equiv -Q_m$ for $t \in [0, t_1)$, $Q(t) \equiv Q_m$ for $t \in [t_1, t_2)$, $Q(t) \equiv -Q_m$ for $t \in [t_2, t_3)$ and $Q(t) \equiv F_d$ for $t \geq t_3$. The instant when the contact force F_c might decrease to zero is denoted by t_c (see Fig. 6). The critical case of no loss of contact is a kind of grazing where $F_c(t_c) = 0$ and the contact force has a local minimum, that is, $\dot{F}_c(t_c) = 0$, too. In accordance with (4), these conditions provide two equations,

$$k x_2(t_c) + c \dot{x}_2(t_c) = 0 \tag{20}$$

for the two unknowns t_c and v_a. One can solve these equations numerically, when $x_2(t)$ is substituted from (19), in which t_1 and v_a are given by (19) and (18). In order to identify the missing

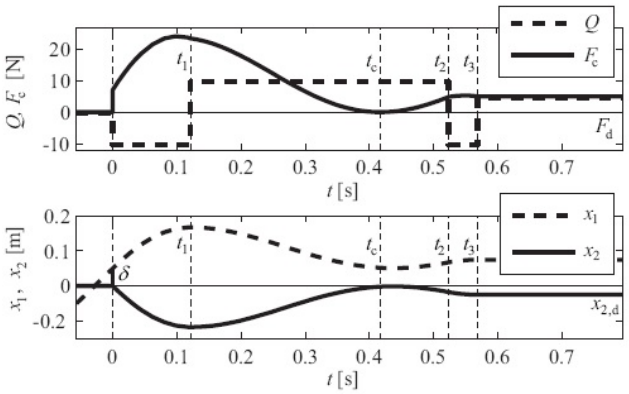

Fig. 6. Control strategy with four steps, parameters $m = 1$ kg, $k = 100$ N/m, $c = 2$ Ns/m, $F_d = 5$ N, $x_{2,d} = -0.05$ m, $\delta = 0.1$ m, $t_1 = 0.121$ s, $t_c = 0.417$ s, $t_2 = 0.523$ s, $t_3 = 0.568$ s, $v_a = 3.541$ m/s.

time instants t_2 and t_3, the continuity conditions of $x_2(t)$ are used at t_2. Consequently, the differential equation (2) is solved for the interval $[t_2, t_3)$ with the initial condition $x_2(t_2)$ and $\dot{x}_2(t_2)$ calculated from (19):

$$x_2(t) = f_0 + (x_2(t_2) - f_0) e^{-\zeta\omega_n(t-t_2)} \times \left(\left(\frac{\zeta\omega_n}{\omega_d} + \frac{\dot{x}_2(t_2)}{(x_2(t_2) - f_0)\omega_d} \right) \sin(\omega_d(t - t_2)) + \cos(\omega_d(t - t_2)) \right). \tag{21}$$

Tab. 1. Summary of the results, velocity of approach v_a, switching times t_1, t_2 and t_3 in case of different control strategies.

No. of steps	v_a [m/s]	t_1 [s]	t_2 [s]	t_3 [s]
1	0.579	0.148	-	-
2	1.188	0.082	-	-
3	2.741	0.114	0.429	-
4	3.541	0.121	0.523	0.568

With this solution and with its time derivative, we obtain two equations,

$$x_2(t_3) = x_{2,d},\ \dot{x}_2(t_3) = 0 \tag{22}$$

for the two unknowns t_3 and t_2. The corresponding numerical values are presented in Fig. 6. The velocity of approach is maximized at 3.541 m/s, and the corresponding switching times define the bang-bang-like computed torque function. The results are summarized in Tab. 1.

4 Conclusions

The approach-and-touch process was analysed in case of stiff targets with low damping and/or inaccurate position feedback. In these cases the approach phase takes the relevant part of the transition time. A time-optimal open-loop control strategy was designed with respect to the length of the approach phase, and the corresponding bang-bang-like computed-torque was calculated for the contact phase. The maximum velocity of approach can be achieved in case of a four-step scenario, but this includes a grazing before the desired contact force is reached.

Note that the approach-and-touch process considered here aimed to model robotic applications. As discussed in [9], the human strategy is different in the sense that our fingers provide large damping, even in case of stiff targets, we cannot use piecewise-constant bang-bang control because of the characteristics of muscles, while we also experience the contact position offset δ due to the finite sensitivity of our position detection. There are similarities in the control strategies, but the measurement results in [9] showed that human muscle activity can be observed even before the contact occurs. Further analysis of the approach-and touch process may lead to improved robotic applications.

References

1 **Nagata F, Hase T, Haga Z, Omoto M**, *CAD/CAM-based position/force controller for a mold polishing robot*, Mechatronics **17** (June 2007 May), no. 4–5, 207–216, DOI 10.1016/j.mechatronics.2007.01.003.

2 **Huang H, Gong ZM, Chen XQ, Zhou L**, *Robotic grinding and polishing for turbine-vane overhaul*, Journal of Materials Processing Technology **127** (30 September 2002), no. 2, 140–145, DOI 10.1016/S0924-0136(02)00114-0.

3 **Bahar BG, Vakarelski IU, Moudgil BM**, *Role of interaction forces in controlling the stability and polishing performance of CMP slurries*, Journal of Colloid and Interface Science **263** (15 July 2003), no. 2, 506–515, DOI 10.1016/S0021-9797(03)00201-7.

4 **Liao L, Xi FJ, Kefu L**, *Modeling and control of automated polishing/deburring process using a dual-purpose compliant toolhead*, International Journal of Machine Tools and Manufacture **48** (October 2008), no. 12–13, 1454–1463, DOI 10.1016/j.ijmachtools.2008.04.009.

5 **Stépán G, Steven A, Maunder L**, *Dynamics of robots with digital force control*, in Proceedings of CSME Mechanical Engineering Forum 1990, 3, (Toronto, 1990), pp. 355–360.

6 **di Bernardo M, Budd CJ, Champneys AR, Kowalczyk P**, *Piecewise-smooth Dynamical Systems:Theory and Applications*, 2008.

7 **Kollár L, Stépán G, Turi J**, *Dynamics of piecewise linear discontinuous maps*, International Journal of Bifurcation and Chaos **14** ((2004)), no. 7, 2341–2351, DOI 10.1142/S0218127404010837.

8 **Mugge W, Schuurmans J, Schouten AC, van der Helm CT**, *Sensory Weighting of Force and Position Feedback in Human Motor Control Tasks*, The Journal of Neuroscience **17** (April 29), 5476–5482, DOI 10.1523/JNEUROSCI.0116-09.2009.

9 **Venkadesan M, Valero-Cuevas FJ**, *Effects of neuromuscular lags on controlling contact transitions*, Phil. Trans. R. Soc. A **367** (28 March 2009), no. 1891, 1163–1179, DOI 10.1098/rsta. 2008.0261.

10 **Pontryagin LS**, *The Mathematical Theory of Optimal Processes*, Interscience **4** (1962).